Local fracture behavior and integrity assessment of a dissimilar metal welded joint in nuclear power systems

Guozhen Wang*, Haitao Wang, Fuzhen Xuan, Shantung Tu

Key Laboratory of Pressure Systems and Safety, Ministry of Education, East China University of Science and Technology, Shanghai 200237, China
* Corresponding author: gzwang@ecust.edu.cn

Abstract In this paper, fracture tests and microscopic observations were conducted on an Alloy52M dissimilar metal welded joint (DMWJ) between A508 ferritic steel and 316L stainless steel in nuclear power systems. The local fracture behavior in the DMWJ was investigated, and the significance of using local fracture resistance in integrity assessment of the DMWJ was analyzed. The results show that the local fracture resistance in the DMWJ is determined by the local fracture behavior, and which is mainly related to the microstructure and local strength mismatch of materials at the crack locations. The crack growth always deviates to the materials with lower strength, and the crack path deviations are mainly controlled by the local strength mismatch. If the local fracture resistance properties could not be obtained and used for cracks in heat affected zone (HAZ), interface and near interface zone, the use of the J-resistance curves of base metals or weld metals following present codes will unavoidably produce non-conservative (unsafe) or excessive conservative assessment results. In most cases, the assessment results will be potentially unsafe. Therefore, it is recommended to obtain and use local mechanical and fracture resistance properties in the integrity assessment of DMWJs.

Keywords Local fracture behavior, Dissimilar metal welded joint, Integrity assessment, Strength mismatch, Crack growth path

1. Introduction

In primary water systems of pressurized water reactors (PWRs)，low alloy ferritic steel is specifically selected to manufacture the nuclear pressure vessels for its high toughness and economical interest, while austenitic stainless steel is selected to make primary pipes for its proper strength and good corrosion resistance. In order to join the ferritic steel pipe-nozzles of the pressure vessels to the austenitic stainless steel pipes well, a transitional stainless steel safe-end pipe is usually introduced. A dissimilar metal welded joint (DMWJ) is usually utilized to join the pipe nozzle with the safe end pipe, as shown in Fig.1. Nevertheless, the welds were indicated to be vulnerable components from the international surveys, owing to their proneness to different types of flaws. Axial and circumferential defects within DMWJs caused by stress corrosion or fatigue have been found in the nuclear power plants (NPPs) in many countries [1-2]. In addition, serious leakage events on such DMWJs have also been reported [3-4]. Thus, maintaining integrity of such joints in case of defect presence and structure overloading is critical to ensure their safe service. To do this, an accurate structural integrity assessment for such DMWJ structure is very important.

Understanding local fracture behavior on the critical regions of such welded joints is essential for conducting an accurate integrity assessment and design. However, due to highly inhomogeneous nature across the DMWJ in terms of microstructure, mechanical, thermal and fracture properties, it is difficult to conduct analytical or experimental fracture investigations on the DMWJs. Only there are limited studies on the fracture behavior of the DMWJs in the literature[5-8]. In addition, in the integrity assessment methods for weld joints in existing codes, such as R6[9], SINTAP and FITNET FFS [10], the weld joints are often simplified as a sandwich composite composed of base metal and weld metal, and the effects of the interface fusion regions between different materials and heat affected zones (HAZs) are usually ignored. In fact, defects in welded structures can occur anywhere, such as in the fusion zone, HAZ, weld, near weld, interface region, base metal, etc. The use of adequate and precise material input parameters (based on the experimental observation of the local damage and fracture process in the joint area) is particularly essential to describe and predict the

critical condition in welded structures [10]. Therefore, the local fracture behavior of the DMWJs should be investigated and understood.
In this study, the local fracture behavior in a real Alloy52M dissimilar metal welded joint between A508 ferritic steel and 316L stainless steel in NPPs were investigated by using the single-edge notched bend (SENB) specimens. The significance of using the local fracture properties in integrity assessment of DMWJs was analyzed.

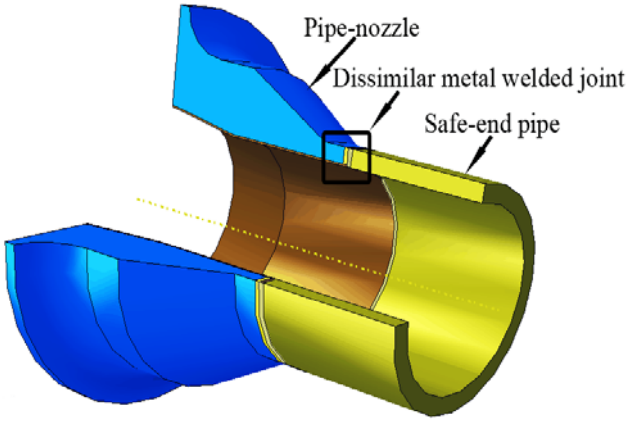

Figure 1. The DMWJ structure for connecting the pipe-nozzle of a reactor pressure vessel to safe-end pipe

2. Experimental procedures

2.1 Materials and fabrication of the DMWJ

A full scale mock up of the DMWJ was fabricated by Shanghai Company of Nuclear Power Equipment in China. The pipe-nozzle material is ferritic low-alloy steel (A508), and the safe end pipe material is austenitic stainless steel (316L). The weld was manufactured by applying a buttering technique and the buttering material as well as weld material is the same nickel-base alloy (Alloy52M), but their manufacture procedures were different. The buttering layer was deposited through an Alloy52M welding wire by automatic gas-tungsten arc welding (GTAW) on the ferritic nozzle face. Then a heat treatment was conducted on the buttering to relieve the residual stress. This buttering layer material is denoted as Alloy52Mb. After buttering, welding was carried out between the buttering layer and the austenitic safe-end pipe by using the GTAW, and the Alloy52M welding wire was also used. Here, this weld metal material is denoted as Alloy52Mw.

2.2 Specimen geometry and crack locations

The single-edge notched bend (SENB) specimen was used for measuring the local fracture properties and observing fracture mechanism in the DMWJ. The SENB specimens with different crack locations were extracted by electric discharge machining from the DMWJ. The initial crack locations and specimen orientation are shown in Fig.2. The cracks 1 and 13 are located in the base metal A508 and 316L, respectively. The cracks 5 and 9 are located in the center of the butter Alloy52Mb and weld Alloy52Mw, respectively. Other cracks are mainly located in the interface regions between materials with complex metallurgical microstructures and inhomogeneous mechanical properties. The interface region cracks include the HAZ cracks in base metals (cracks 2, 6 and 12), interface cracks at fusion lines (cracks 3, 7 and 11), and the near interface zone (NIZ) cracks in weld metals (cracks 4, 8 and 10). The distance of the HAZ and NIZ cracks from the interfaces is 1.5mm. The SENB specimen geometry, size and loading method are typically shown in Fig.3 for the crack 4 specimen.

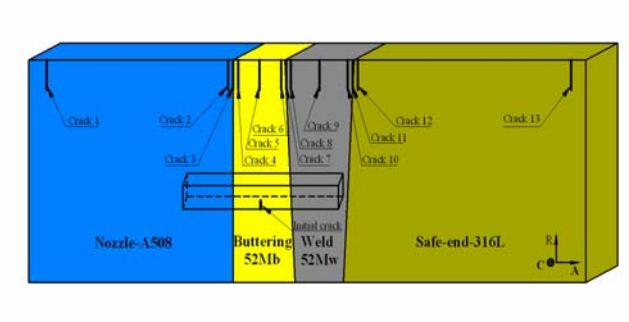

Figure 2. Schematic diagram showing initial crack positions and SENB specimen orientation in the DMWJ (C: circumferential, R: radial direction, A: axial direction)

2.3 Experiments and observations

The fracture tests of the SENB specimens were performed by an Instron screw-driven machine at room temperature. One specimen was tested for every crack location. The quasi-static loading was conducted by displacement controlled mode at a cross-head speed of 0.5mm/min. The load-load line displacement curves were automatically recorded by a computer aided control system of the testing machine. The single specimen method and the normalization technique conforming the ASTM E1820 procedure [11] were used to obtain the J-resistance curve for each specimen. After testing, the tested specimens with a certain crack growth length were sectioned at the mid-plane. One of the cut pieces was polished and etched to reveal damage and fracture patterns in microstructure ahead of the crack tip, which was observed by an optical microscope (OM) and a scanning electron microscope (SEM). Another piece was broken, and the initial crack length and the final crack growth length were measured and the fracture surfaces were observed with the SEM to understand the failure mechanism.

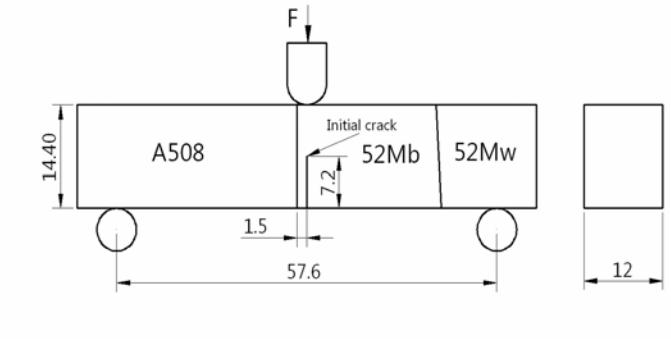

Figure 3. The SENB specimen geometry, size and loading method typically shown by the crack 4 specimen

3. Results and discussion

3.1 Local fracture properties of the DMWJ

The J-resistance curves of the SENB specimens with various crack positions are given in Fig.4. These J-resistance curves reflect local crack growth resistance of different material regions in the DMWJ. It can be seen that the three cracks (cracks 1-3) in A508 region and the two cracks (cracks 9 and 10) in weld Alloy52Mw region have lower crack growth resistance, and which represents local weak zones for fracture in the DMWJ. The fracture resistance of crack 3 at A508/Alloy52Mb interface is lowest. The J-resistance curves of crack 5 in the center of buttering Alloy52Mb and crack 13 in the base metal 316L are highest, and they represents the highest fracture resistance zones in the joint. The J-resistance curves of other cracks (cracks 4, 6, 7, 8, 11 and 12) are located

between the lower crack growth resistance curves (cracks 1,2,3,9 and 10) and the highest crack growth resistance curves (cracks 5 and 10). The cracks 6, 7 and 12 have similar resistance curves. The resistance curves of cracks 4, 8 and 11 are also basically the same, but they are lower than those of the cracks 6, 7 and 12. The local crack growth resistance in the DMWJ is determined by fracture mechanism occurring ahead of the crack tip, and which is mainly related to the microstructure and local strength mismatch of materials at the crack location. This will be analyzed in the following sections.

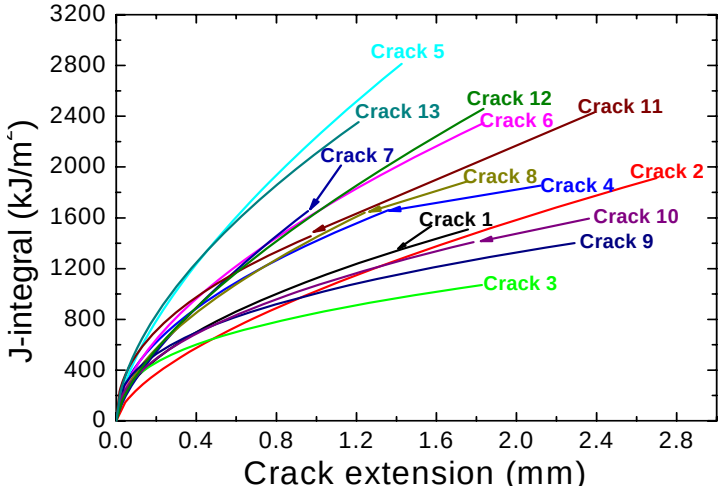

Figure 4. J-resistance curves for the 13 cracks in the DMWJ

3.2 Fracture behavior of typical cracks in the DMWJ

Because of the microstructual and mechanical heterogeneities along the DMWJ, the cracks located in different regions in the DMWJ will have different fracture behavior and leads to different local fracture properties. This can be analyzed as follows.

Fig.5 shows the fracture surface and crack growth path of the A508 HAZ crack 2. Fig.5(a) shows an overview of the fracture surface. In the area A marked in Fig.5(a) in front of initial fatigue precrack, the brittle flat fracture appearance can be seen, as shown by Fig.5(b). This indicates that local brittle fracture initiats and propagates from the the initial fatigue pre-crack tip. In the area B marked in Fig.5(a), a large amout of shollow dimples can be seen, as shown by Fig.5(c). This shows that local ductile fracture has occurred there. Because the area B is behind the area A, this implies that the fracture mode in the crack 2 specimen firstly is brittle fracture, and than changes into ductile fracture. This change in fracture mode also can be observed from the crack growth path shown in Fig.5(d). On the first crack growth length of about 1mm, edges of the crack path are flat, and this is a characteristic of brittle fracture. On the later crack growth path, irregular crack edges can be seen, and this is a characteristic of ductile fracture. This crack path deviation also can be seen by the change of fracture surface from flat (zone I) to rough (zone II) in Fig.5(a). Fig.5(d) also shows that the crack 2 has a deviation path towards A508 base metal (away from the A508/Alloy52Mb interface). The initial brittle fracture of crack 2 is related to the dominated martensite microstructure with higher strength in A508 HAZ. The high strength martensite microstructure generally has low fracture toughness, and the brittle fracture tends to occur under higher crack-tip opening stress. In addition, the A508 HAZ has steep strength gradient, as shown in Fig.6. The left side of crack 2 is near the A508 base metal, and has lower strength (Fig.6). The local higher plastic strain and stress triaxiality will occur at the left side of crack 2, which will induce the crack 2 to grow towards its left side [10]. This crack path deviation may promote the change of fracture mode from the brittle fracture to the ductile fracture. This comes from two factors. One factor is that the crack path

deviation makes the mode I crack change into mixed crack of mode I and II, and this reduces the driving stress for brittle fracture (crack-tip opening stress). Another factor is that the crack path deviates to the material with lower strength (may have higher toughness), and larger plastic deformation may relax local crack-tip opening stress, which can promote development of ductile fracture process. The mixed mechanism of brittle and ductile fracture in the crack 2 specimen leads to the lower fracture resistance curve (Fig.4). In this case, the resistance curve only reflects apparent fracture resistance of A508 HAZ due to the change of fracture mechanism and crack growth path deviation which is mainly related to the local strength mismatch.

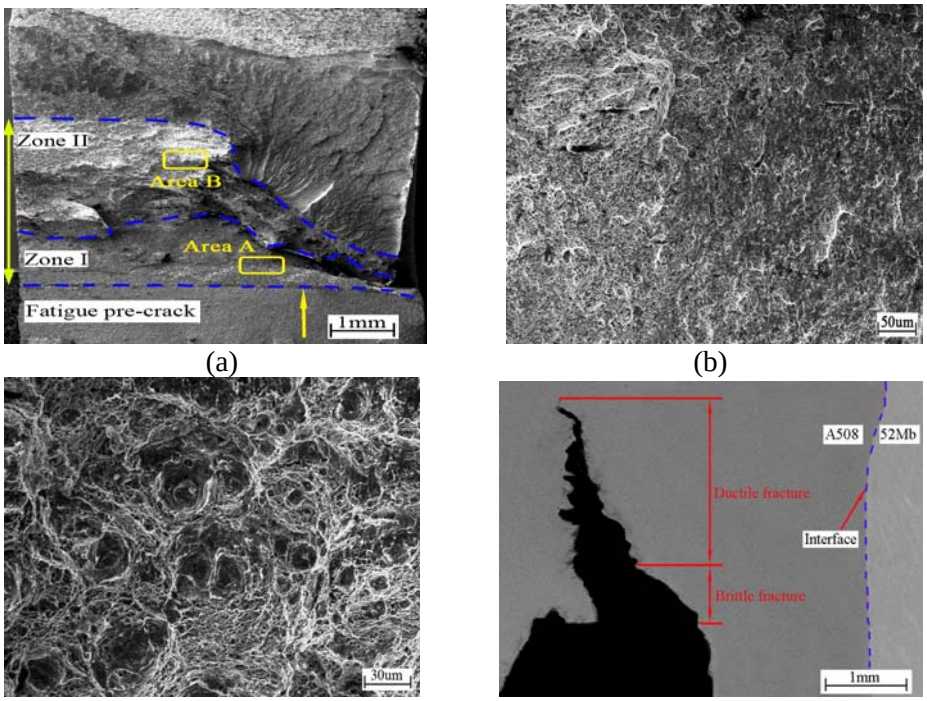

Figure 5. SEM images show fracture mechanism of the A508 HAZ crack 2. (a) overview of fracture surface, (b) higher magnification of area A in (a), (c) higher magnification of area B in (a), (d) crack growth path.

Fig.7 shows the crack growth path and fracture surface of A508/52Mb interface crack 3. It can be observed from Fig.7 (a) that the crack path deviates to the side of 52Mb with lower strength (Fig.6). The fracture surface in Fig.7 (b) displays a large amount of brittle facets with some shallow dimples. This implies that the fracture mechanism of A508/52Mb interface crack 3 is mixed brittle and ductile fracture, but is dominated by brittle fracture. This predominantly brittle fracture may result from two factors. One factor is the local strength mismatch of materials at two sides of crack 3. The essence of the strength mismatch lies on the crack tip plasticity development and effect of the strength difference between different local regions on the deformation pattern ahead of the crack tip [10]. The strength mismatch affects the constraint conditions and stress levels near the crack tip, hence affects the fracture mechanism and crack growth path inevitably. For the A508/52Mb interface crack 3, the Alloy52Mb side has lower strength than the A508 side (Fig.6). During loading the crack 3 specimen, the plastic deformation will firstly appear in the Alloy52Mb material near the interface, and higher stress triaxiality, opening stress and plastic strain will be induced in the Alloy52Mb side with increasing applied load. This has been confirmed by the finite element analyses in the Ref. [13]. The higher stress triaxiality and opening stress will promote development of the brittle fracture with little ductility, and make the crack path deviate towards the Alloy52Mb side. Another factor for producing the predominantly brittle fracture is the predominant martensite microstructure with high strength and low toughness in the A508/52Mb interface region. It can be concluded that the predominantly brittle fracture mechanism causes the lowest J-resistance curve of

the A508/52Mb interface crack 3 (Fig.4). The A508/52Mb interface region is the weakest zone for failure in the DMWJ.

Typical damage patterns ahead of crack tips for the cracks in Alloy52Mb and 52Mw are shown in Fig.8. It can be found that there are a lot of voids distributed on the grain boundarys of columnar crystals near crack, and some grain boundary cracks also have been formed by coalescence of voids. It is believed that the grain boundarys are weak zones for damage and fracture in the weld metals. The crack growth direction is approximately perpendicular to the transverse columnar crystals in buttering Alloy52Mb, but it is approximately parallel to the lognitudinal columnar crystals in weld Alloy52Mw. Fig.8(a) shows that the crack in Alloy52Mb propagtes across the transverse columnar crystal boundary, while Fig.8(b) shows that the crack in Alloy52Mw propgates along the lognitudinal columnar crystal boundary. The columnar crystal orientation relative to crack growth direction apparently affects fracture mechanism and crack growth resistance. For the cracks in buttering Alloy52Mb, the direcrion of the maximum crack-tip opening stress is parallel to columnar crystal boundaries, and the stress normal to the grain boundaries is too low to drive damage and fracture along weak grain boundaries. It needs much high driving force to propagate a crack across columnar crystals, thus the crack growth resistance is high. But for the cracks in weld Alloy52Mw, the direcrion of the maximum crack-tip opening stress is perpendicular to columnar crystal boundaries, and it is ease to drive damage and fracture developing along weak grain boundaries, thus the crack growth resistance is low.

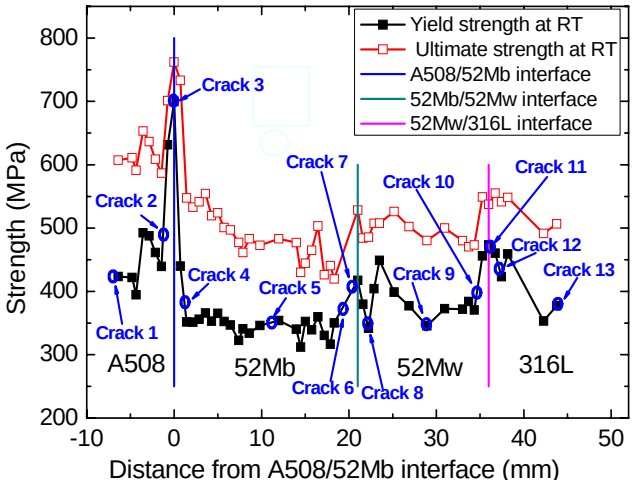

Figure 6. The strength distributions [12] and crack positions across the DMWJ.

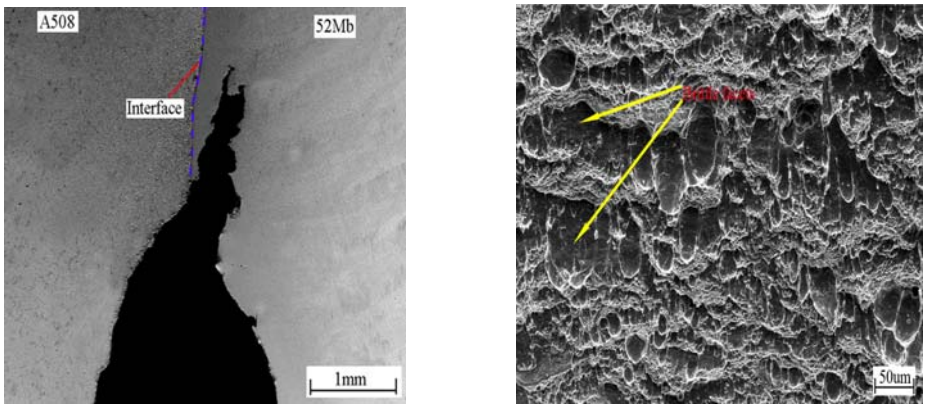

(a) (b)

Figure 7. Crack growth path (a) and fracture surface (b) of A508/52Mb interface crack 3

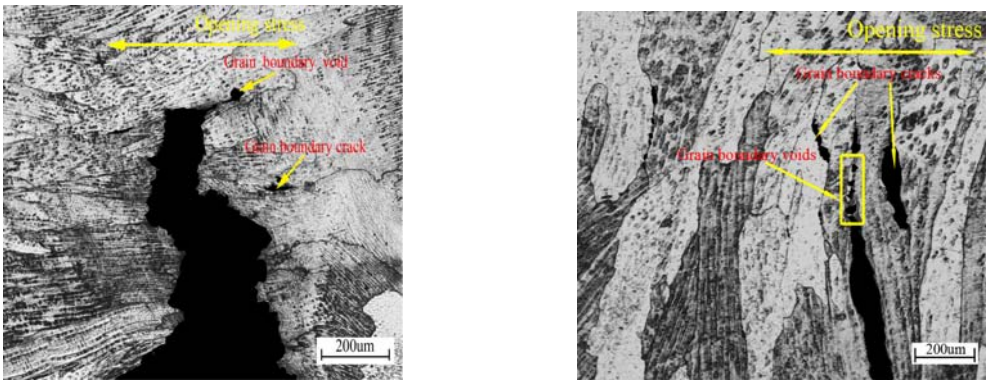

(a) (b)

Figure 8. Typical damage patterns ahead of crack tips for the cracks in Alloy 52Mb (a) and 52Mw (b)

3.3 Integrity assessment for the DMWJ structure

Although there are many methodologies for structural integrity assessment, the failure assessment diagram (FAD) is extremely simplified and convenient which is in the realm of elastic-plastic fracture mechanics. However, the use of the FAD for the DMWJ structure in nuclear power plants is a challenge due to the highly heterogeneous microstructure, mechanical and fracture properties along the joint. When the initial cracks are located at different positions (such as base metal, buttering, weld, interfaces region, HAZ, NIZ, etc.), the crack-tip plastic deformation, damage and further crack growth can occur in any materials and even the crack growth path may change from one material to the other, as shown in Figs. 5(d) and 7(a). In these cases, the crack-tip fracture parameter and plastic deformation behavior of the structure is difficult to define due to the complex strength mismatch effect in the DMWJ, thus the general FADs in current codes cannot be directly and accurately used. It has been found that the strength mismatches in similar metal weld joints have significant effects on the crack driving force, limit load and failure assessment curve [14, 15]. At present, simplified engineering integrity assessment methods have been developed for treating the problem of weld joints, and the concept of equivalent material properties is utilized so that the integrity assessment method for single material can be used for the joints [16-18]. However, the effects of the crack locations and related local strength mismatches in the DMWJ on the local fracture resistance, crack growth paths, failure assessment curves and structural deformation behavior have not been completely understood and accurately taken into account in FADs, and no specific accurate methods exist for the integrity assessment of the complex DMWJ.

In the integrity assessment methods for weld joints in existing codes, such as R6[9], SINTAP and FITNET FFS [10], the joints are often simplified as a sandwich composite composed of base metal and weld metal, and the effects of the interface region, HAZ and NIZ are ignored. In fact, defects in welded structures can occur anywhere, including in base, weld, near weld, HAZ, fusion zone, interface region, etc. The selection of strength and toughness values to be used in the integrity assessment of welded structures has significant implications on the outcome of the analysis. The use of adequate and precise input parameters (based on the experimental observation of the local damage and fracture process in the joint area) is particularly essential to describe and predict the critical condition in such structures [10]. According to the present codes, in the integrity analysis and assessment for the DMWJ structure, the DMWJ will be simplified as a composite composed of four materials (A508 steel, buttering Alloy52Mb, weld Alloy52Mw and 316L stainless steel). For the cracks located in various positions in the DMWJ, only the mechanical and fracture properties of the four materials are used. For the HAZ, interface region and NIZ cracks, if only the mechanical and fracture properties of base metals (A508, 316L) or the weld metal (buttering Alloy52Mb, weld Alloy52Mw) are used, non-conservative (unsafe) or excessive conservative results will then be potentially produced. This can be analyzed as follows for the DMWJ.

To conduct the ductile tearing assessment and leak-before-break (LBB) analysis, a ductile crack growth instability evaluation based on elastic-plastic fracture mechanics should be performed under a maximum loading condition, and a ductile crack growth resistance curve of a material is needed. For the cracks in A508 region, it can be estimated from Fig.4 that if the J-resistance curve of the A508 base metal (crack 1) is used to assess the A508 HAZ crack 2 and the A508/Alloy52Mb interface crack 3, slight non-conservative and unsafe result will be produced, respectively. This is due to that the J-resistance curve of cracks 2 and 3 is slight lower and lower than that of the A508 base metal crack 1, respectively. For the cracks in buttering Alloy52Mb region, it can be judged from Fig.4 that if the J-resistance curve of the buttering Alloy52Mb (crack 5) is used to assess the interface crack 3, NIZ crack 4, HAZ crack 6 and interface crack 7, non-conservative (unsafe) results will be produced due to the highest J-resistance curve of the buttering Alloy52Mb. Especially for the A508/Alloy52Mb interface crack 3 with local crack growth into the Alloy52Mb, the use of the J-resistance curve of the Alloy52Mb will lead to the extreme unsafe result. For the cracks in weld Alloy52Mw region, it can be predicted from Fig.3 that if the J-resistance curve of the weld Alloy52Mw (crack 9) is used to assess the interface crack 7, NIZ crack 8 and interface crack 11, it will lead to excessive conservative assessments. While the use for the NIZ crack 10 will be reasonable due to the similar J-resistance curve of cracks 9 and 10. For the cracks in 316L region, it can be estimated from Fig.4 that if the higher J-resistance curve of the base metal 316L (crack 13) is used to assess the interface crack 11 and HAZ crack 12 with lower J-resistance curve, non-conservative (unsafe) results will be obtained.

In general, the analyses described above demonstrate that without considering the local fracture resistance properties of narrow HAZ, interface region and NIZ , the use of the J-resistance curves of base metals (A508 and 316L) or the weld metals (buttering Alloy52Mb and weld Alloy52Mw) will unavoidably produce non-conservative (unsafe) or excessive conservative assessment results. In most cases, the assessment results are potentially unsafe. A recent study [19] has shown that the resistance to crack initiation and growth is greatly affected by the heterogeneity of the weldment, and the importance of the HAZ for fracture behavior of welded joints was also emphasized. Therefore, in the integrity assessment for the DMWJ structure, it is recommended to obtain and use local mechanical and fracture resistance properties of all regions of the joint if the complex local mismatch situation is a concern. The new integrity assessment methods based on local damage and fracture models also need to be developed for the DMWJs.

4. Conclusion

(1) The local fracture properties in the DMWJ are determined by fracture mechanism occurring ahead of the crack tip, and they are mainly related to the microstructure and local strength mismatch of materials at the crack locations.

(2) The fracture mechanism of A508 HAZ crack 2 and A508/52Mb interface crack 3 is a mixed brittle and ductile fracture, which is related to strength mismatch and predominant martensite microstructure. This fracture behavior leads to the lower crack growth resistance.

(3) The columnar crystal orientation relative to crack growth direction apparently affects fracture behavior and crack growth resistance of cracks in buttering Alloy52Mb and weld Alloy52Mw. The cracks in Alloy52Mb propagate across columnar crystals in a ductile mode, thus higher crack growth resistance is produced. While the cracks in weld Alloy52Mw mainly propagate along columnar crystal boundaries with low resistance in a brittle mode, which leads to lower crack growth resistance.

(4) The crack path deviations are observed for most cracks in the interface regions, HAZs and NIZs. The cracks always deviate to the materials with lower strength, and the crack path deviations are mainly controlled by strength mismatch.

(5) If the local fracture resistance properties could not be used for the heat affected zone (HAZ),

interface and near interface zone cracks, the use of the J-resistance curves of base metals (A508 and 316L) or the weld metals (buttering Alloy52Mb and weld Alloy52Mw) will unavoidably produce non-conservative (unsafe) or excessive conservative assessment results. In most cases, the assessment results will be potentially unsafe.

(6) In the integrity assessment for the DMWJ structure, it is recommended to obtain and use local mechanical and fracture resistance properties of all regions of the joint if the complex local mismatch situation is a concern. The new integrity assessment methods based on local damage and fracture models also need to be developed for the DMWJs.

Acknowledgement

This work was financially supported by the Projects of the National Natural Science Foundation of China (51075149), the National High Technology Research and Development Program of China (2012AA040103), and the Fundamental Research Funds for the Central Universities of China.

References

[1] C. Jang, J. Lee, J.S. Kim, Mechanical property variation within Inconel 82/182 dissimilar metal weld between low alloy steel and 316 stainless steel. Int J Press Ves Pip, 85(2008) 635–646.

[2] J.W. Kim, K. Lee, J.S. Kim, Local mechanical properties of Alloy 82/182 dissimilar weld joint between SA508 Gr.1a and F316 SS at RT and 320℃. J Nual Mater, 384(2009) 212–221.

[3] PWR Material Realiability Project, Interim Alloy 600 Safety Assessment for U.S. PWR Plants, Part 1: Alloy82/182 pipe butt welds. EPRI Report TP-1001491, 2001.

[4] R. Celin, F. Tehovnik, Degradation of a Ni-Cr-Fe alloy in a pressurised water nuclear power plant. Mater Technol, 45(2011)151-157.

[5] K.H. Schwalbe, A. Cornec, D. Lidbury, Fracture mechanics analysis of the BIMET welded pipe tests. Int J Pres Ves Pip, 81(2004)251-277.

[6] C. Faidy, G. Martin, N. Taylor. Nuclear science and technology. Assessment of Aged Piping Dissimilar Metal Weld Integrity (ADIMEW) final report. European commission. 2008. Eur23315.

[7] M.K. Samal, M. Seidenfuss, E. Roos, K. Balani, Investigation of failure behavior of ferritic-austenitic type of dissimilar steel welded joints. Eng Fail Anal, 18(2011) 999-1008.

[8] A. Laukkanen, P. Nevasmaa, U. Ehrnsten, R. Rintamaa. Characteristics relevant to ductile failure of bimetallic welds and evaluation of transferability of fracture properties. Nucl Eng Des, 237(2007)1-15.

[9] R6, Assessment of the integrity of structures containing defects, Procedure R6-Revision 4. Gloucester: Nuclear Electric Ltd. 2007.

[10] M. Kocak. Structural Integrity of welded structures: Process-Property-Performance (3P) Relationship. 63rd Annual Assembly & International Conference of the International Institute of Welding. 2010, Istanbul, Turkey.

[11] ASTM E1820-08a. Standard test method for measurement of fracture toughness. Philadelphia: American Society for Testing and Materials, 2008.

[12] H.T. Wang, G.Z. Wang, F.Z. Xuan, C.J. Liu, S.T. Tu. Local mechanical properties and microstructure of Alloy52M dissimilar metal welded joint between A508 ferritic steel and 316L stainless Steel. Adv Mater Res, 509(2012)103-110.

[13] H.T. Wang, G.Z. Wang, F.Z. Xuan, S.T. Tu. Numerical investigation of ductile crack growth behavior in a dissimilar metal welded joint. Nucl Eng Des, 241(2011)3234-3243.

[14] M. Zhang, Y.W. Shi, X.P. Zhang. Influence of strength mis-matching on crack driving force and failure assessment curve of weldment. Int J Pres Ves Pip, 70(1997)33-41.

[15] T.K. Song, Y.J. Kim, J.S. Kim, T.E. Jin. Mismatch limit loads and approximate *J* estimates for tensile plates with constant-depth surface cracks in the center of welds. Int J Fract, 148(2007)343-360.

[16] K.H. Schwalbe, U. Zerbst, The Engineering treatment model. Int J Pres Ves Pip, 77(2000) 905–918.
[17] Y.J. Kim, K.H. Schwalbe, Mis-match effects on plastic yield loads in idealized weldments. Engng Fract Mech, 68(2001)163–182.
[18] I.A. Khana, V. Bhasin, An estimation procedure to evaluate limit loads of bi-metallic specimens. Int J Pres Ves Pip, 81(2004)451–462.
[19] B. Younise, A. Sedmak, M. Rakin, Micromechanical analysis of mechanical heterogeneity effect on the tearing of weldments. Mater Des, 37(2012)193-201